Structure of Chemically End-Grafted Polymer Chains Studied by Scanning Force Microscopy in Bad-Solvent Conditions

V. Koutsos, E. W. van der Vegte, E. Pelletier, A. Stamouli, and G. Hadziioannou*

Department of Polymer Chemistry and Materials Science Centre, University of Groningen, Nijenborgh 4, 9747 AG Groningen, The Netherlands

Received November 4, 1996; Revised Manuscript Received April 9, 1997[⊗]

ABSTRACT: In this paper, we study the polymer conformation of chemically end-grafted polymer chains in bad-solvent conditions using a scanning force microscope. The polymer layers were prepared by exposing a gold substrate in a dilute toluene solution of thiol-terminated polystyrene (PS-SH). Although the adsorption process took place in good-solvent conditions, the imaging was performed in water (bad solvent for polystyrene chains). For short incubation times and low concentrations, we identified individual polymer chains. For longer incubation times (higher surface coverage), we observed microphase separation of the polymer monolayer into globular clusters. Using different molecular weights of PS-SH, we showed that the sizes of these clusters satisfy the scaling laws that were predicted for pinned micelles.

1. Introduction

Ultrathin end-grafted polymer layers play an important role in colloidal stabilization,[1,2] chromatography, adhesion,[3] lubrication, microelectronics, and biocompatibility of artificial organs in medicine.[4] Grafting can be attained either by physisorption (diblock copolymers) or by chemisorption (end-functionalized polymers). In good solvents, densely grafted polymer chains swell and stretch away from the surface forming a uniform layer.[5] Recently, much work has been concentrated on the structure of the end-grafted layers in *bad-solvent* conditions.

Theoretical investigation based on random phase approximation (RPA),[6] RPA combined with numerical mean field analysis,[7] scaling analysis,[8] Monte Carlo (MC),[9] and molecular dynamics (MD) simulations[10] showed that below the Θ temperature and for rather moderate grafting densities the polymer brush undergoes lateral phase microsegregation in the form of dimples or clusters. A scaling analysis has been developed based on comparing the free energy of a homogeneous brush with that of a micelle-like structure.[11,12] This model is more appropriate in the strong segregation limit and implies that many chains fuse to form a compact core which is connected to the surface through the grafted tethers.

Only few experimental studies have been published on this subject. In all of them, the polymer films were investigated by means of scanning force microscopy (SFM).[13] O'Shea et al.[14] used PEO/PS diblock copolymer adsorbed on mica and observed "agglomeration" at monolayer coverage in solvents of different quality. In another study of end-grafted polystyrene chains spun onto silicon substrates, the chains were found to tangle together and form islands.[15] Siqueira et al.[16] using end-functionalized diblock copolymers observed the three theoretically predicted regimes: homogeneous layer, dimples, and isolated islands when the surface coverage was decreased. Recently, Stamouli et al.[17] imaged isolated islands of P2VP/PS diblock copolymer adsorbed onto mica from toluene. They observed polymer segregation in well-defined clusters and assessed their number density. Assuming that these clusters are pinned micelles and applying the relevant scaling laws, they calculated the mass coverage. This estimated value, based on the pinned micelle model, compared favorably with independent measurements.

In this paper we investigate the conformation of grafted polystyrene chains on vapor-deposited gold surfaces in the strong segregation limit by means of SFM. The polystyrene contains a terminal thiol group and is chemisorbed onto the gold substrate via a gold−thiolate bond from dilute solutions.[18,19] This system allows spontaneous adsorption of end-functionalized polystyrene (PS-SH) from good solvents, where unmodified polystyrene does not adsorb.[19,20] The imaging has been done in water which is a bad solvent for polystyrene chains. Imaging of polymer layers in bad-solvent conditions has been proven to be quite successful[14] due to the strong polymer−polymer attraction which results in an increased structural stability of the layers. The grafting density of the monolayer is not affected by the change of the solvent since the polymer chains are irreversibly chemisorbed onto the gold substrate. We report on two aspects: (1) the structure of the polymer monolayer adsorbed onto gold from very dilute solutions, for short and long adsorption times; (2) the effect of molecular weight on the morphology of the saturated polymer monolayer (fixed incubation times).

2. Experimental Section

2.1. Materials. Toluene p.a. (Merck) was used as received. Styrene (Janssen Chimica) was distilled from calcium hydride at reduced pressure (15 mbar) and stored under nitrogen at −20 °C. Styrene was distilled from dibutylmagnesium at reduced pressure (15 mbar) just prior to use. Tetrahydrofuran (THF, Janssen Chimica), used as a solvent, was dried by Na/benzophenone under argon. It was refluxed until a deep purple color was obtained, indicating dryness, and then collected under argon. Propylene sulfide (Aldrich) was distilled from calcium hydride under argon and stored under argon at −20 °C. Cumylpotassium carbanion was used as a monofunctional initiator.[21] A 0.1 M solution of this initiator was prepared by adding 0.4 g of potassium and 1.4 mL of bis(α-methylbenzyl) ether to 50 mL of dry THF at −20 °C under argon. The colorless solution slowly darkened to deep red. After warming to room temperature, the solution was stirred overnight. Gold wire (Schöne Edelmetalen) was 99.99% pure.

2.2. Synthesis of Thiol-Terminated Polystyrene. Thiol-terminated polystyrene (PS-SH) was prepared by anionic

* To whom correspondence should be addressed.
[⊗] Abstract published in *Advance ACS Abstracts,* June 15, 1997.

S0024-9297(96)01625-7 CCC: $14.00 © 1997 American Chemical Society

Table 1. PS_x−SH[a]

polymer	M_w	M_w/M_n
PS_{400}−SH	41 500	1.09
PS_{500}−SH	51 500	1.1
PS_{800}−SH	85 000	1.2
PS_{1400}−SH	144 000	1.2
PS_{2500}−SH	258 000	1.1

[a] The subscript refers to the approximate degree of polymerization.

polymerization.[19,21] A 250 mL Schlenk tube was filled with 150 mL of dry THF under argon. A sufficient amount of initiator was added to the THF to maintain a pink color while the solvent was cooled to −78 °C by a methanol/acetone bath. This method was used to deactivate impurities which could cause premature termination of the living chains. The appropriate amount of initiator for the desired molecular weight was added at once. Ten milliliters of styrene was added dropwise. At the end of the styrene polymerization reaction the solution was still red, indicating the presence of living chain ends. The polystyryl anions were titrated with propylene sulfide and subsequently protonated with acidic methanol to obtain the thiol-terminated polystyrene (the solution becomes colorless). The polymer was isolated by precipitation in methanol and further purified by repeated dissolution in THF and precipitation in methanol. The molecular weight and the molecular weight distribution of the polymer were determined by gel permeation chromatography (GPC) using a Spectra Physics system P110 pump with autosampler system (Spectra Physics AS1000), PLgel 5μ mixed column, a Shodex RI71 refractive index detector, and a Viscotek H502 viscometer detector. Molecular weight data for all PS_x−SH are given in Table 1.

2.3. Substrate Gold Film Preparation. Mica was cleaved in air and immediately placed in the vacuum chamber of a diffusion-pumped thermal evaporator (Edwards Auto 306). The mica sheets were heated to 400 °C at a pressure below 1×10^{-4} mbar. Gold was evaporated from resistively heated tungsten boats at a pressure below 5×10^{-6} mbar. The thickness of the gold layer was monitored with a quartz crystal oscillator and eventually amounted to 35 nm (deposition rate 3 nm/min). The gold substrates were left at 400 °C for 2 h and then cooled down to room temperature in vacuum. The vacuum chamber was backfilled with prepurified nitrogen, and the gold substrates were removed and stored under nitrogen until further use.

2.4. Sample Preparation. All the samples were prepared by exposing the gold substrates to a toluene solution of the desired concentration of PS-SH.[20] A variety of incubation times was used. The PS-SH concentration in the solution was kept well below the critical overlap concentration c^*.[22] This ensures the grafting of isolated and well-separated polymer chains onto the gold surface. After the desired incubation time, the substrates were removed from the adsorption solution and immediately rinsed exhaustively with fresh toluene. The samples were dried under a stream of argon and were placed in vacuum at 50 °C for 1 h and stored in nitrogen. For the first topic of this study we used a 0.1 mg/mL polymer solution of PS_{1400}−SH and various incubation times (from a few minutes to 24 h). In the discussion we restrict ourselves to differences observed between short and long adsorption times. A chemisorption kinetic study will appear elsewhere.[23] For the second topic, the gold substrates were immersed in 2 mg/mL solutions of PS_x−SH for 48 h. Different molecular weights were used (Table 1). For incubation times longer than 24 h we did not observe any changes. Thus, we conclude that in 24 h the ultimate surface coverage has been achieved. This observation is in aggrement with independent measurements of ref 19. In addition, Stouffer et al.[19] employing liquid scintillation counting (LSC) showed that the maximum mass coverage is approximately 2−3 mg/mL (for similar molecular weights and concentrations with ours).

2.5. Scanning Force Microscopy. All scanning force microscopy experiments have been performed in water (bad solvent for PS-SH molecules) using a Topometrix SFM (Explorer). We imaged the samples in contact mode (tip in contact with the surface) keeping the applied force constant. Commercially available Si_3N_4, V-shaped cantilevers (spring constant 0.032 N/m) were used. The imaging was performed in water in order to eliminate any meniscus forces that can act as an additional load and disturb the measurements.[24,25] In addition, in order to avoid any distortion of the polymer layer, the applied force was kept low. Within the range of −2 nN (applied force ≈ adhesive force) to 5 nN we did not see any changes on the topography values that we report. We deduced the tip radii by SFM images of sharp structures or edges (as described in ref 26). We found an average value of 50 nm, which is equal to that supplied by the manufacturer (Topometrix). For all the measurements that are reported in this study we used the same tip.

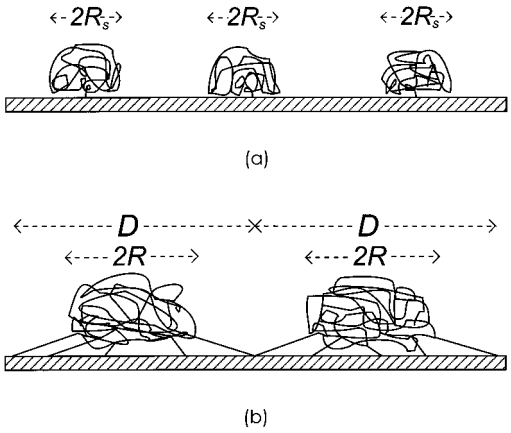

Figure 1. Schematic drawing of (a) isolated collapsed polymer chains sparsely grafted on a substrate and (b) pinned micelles.

Several samples were made for each incubation time and each sample was imaged at different areas. Similar pictures were obtained, demonstrating the reproducibility of the results. All images are shown without any image processing except horizontal leveling.

The particle sizes in AFM images were averaged from line profiles along (at least) four nonparallel directions across the particle image. Care has been taken to exclusively address particles located in flat gold terraces and not near edges or channels, because in the latter case the tip convolution effects are more severe.

3. Theoretical Background

A polymer brush in the strong segregation limit is subjected to two opposing factors: the polymer−polymer attraction and the constraint of the tethers. As a result, the polymer layer organizes itself in well-defined, stable clusters. These clusters are called "surface octopus micelles"[11] or "pinned micelles".[12] In this study we adopt and use the second term.

We present a brief account on the physics associated with the formation of the pinned micelles. A detailed treatment can be found in refs 11 and 12.

Firstly, we consider isolated polymer chains, irreversibly grafted on a surface. In bad-solvent conditions each chain collapses forming a single globule (Figure 1a) of radius $R_s \simeq N^{1/3}$ (the size of the monomer unit is assumed equal to 1 throughout these calculations). The surface free energy of each chain scales as

$$\frac{F_s^{(1)}}{kT} \approx R_s^2 \approx N^{2/3} \qquad (1)$$

At moderate grafting densities σ and in bad-solvent conditions the chains fuse to form globules each con-

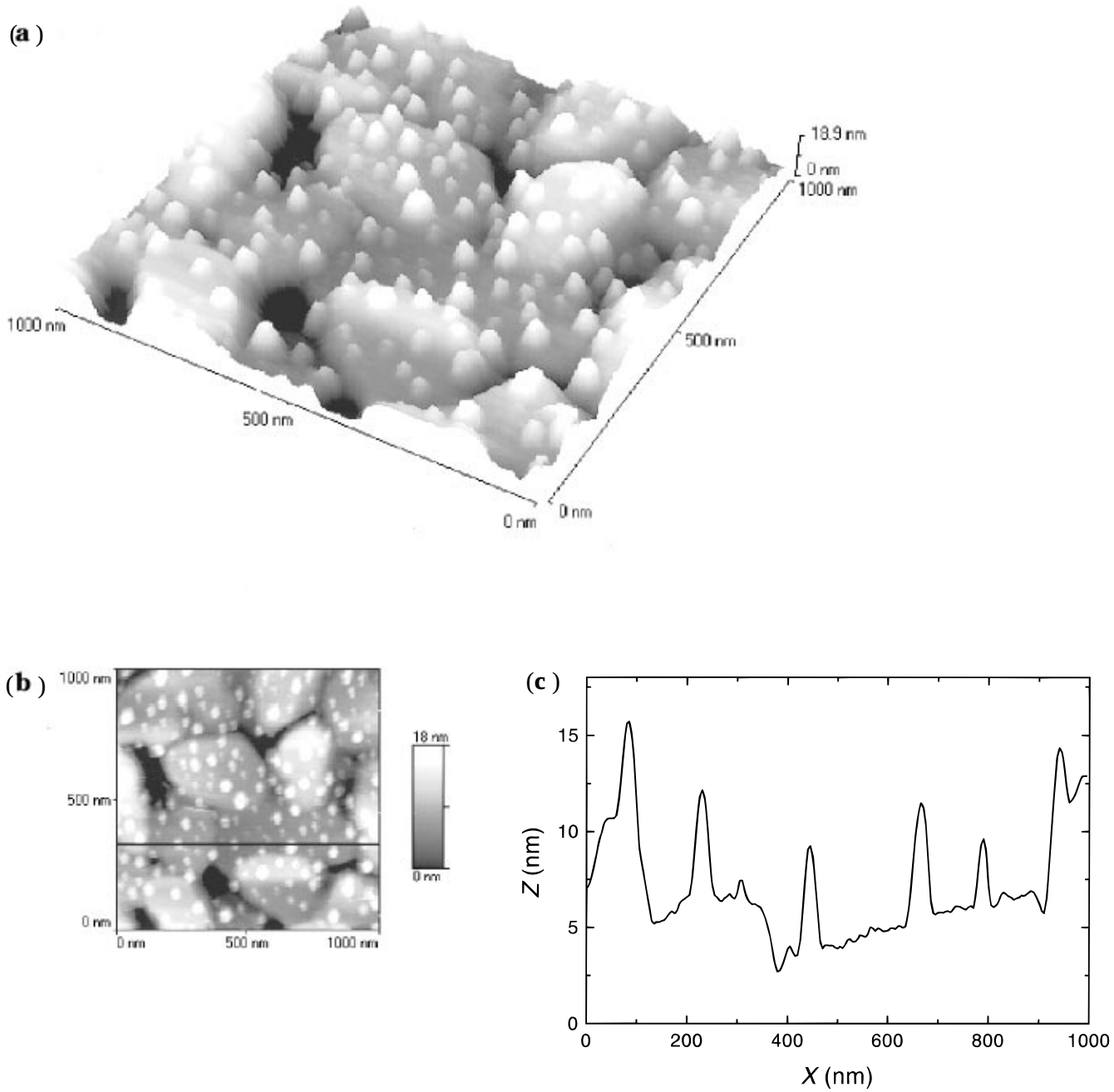

Figure 2. (a) SFM 3D-graph topography image of a gold substrate immersed in a toluene solution of PS_{1400}−SH (concentration, 0.1 mg/mL) for 45 min. The polymer chains are randomly distributed on the gold terraces. (b) Gray scale plot of the same image. (c) Height profile along a typical scan line (black line in (b)). The vertical scaling is different from the horizontal one so the collapsed single chains appear elongated in the z direction.

taining n chains (Figure 1b). The globule consists of a massive core of radius

$$R \approx (nN)^{1/3} \tag{2}$$

which is "pinned" on the surface through tethers. The number of chains within a pinned micelle is

$$n \approx D^2\sigma \tag{3}$$

where D is the characteristic size (extent) of the pinned micelle. The tethers oppose the segregation of the polymers. Their total contribution (stretching energy + surface energy) to the free energy scales as

$$\frac{F_{\text{tether}}}{kT} \approx D \approx n^{1/2}\sigma^{-1/2} \tag{4}$$

The surface energy per chain of a micelle's core scales as

$$\frac{F_s}{kT} \approx \frac{R^2}{n} \approx n^{-1/3}N^{2/3} \tag{5}$$

Thus, the total free energy per chain of a micelle is

$$\frac{F_m}{kT} \approx n^{1/2}\sigma^{-1/2} + n^{-1/3}N^{2/3} \tag{6}$$

By minimizing this free energy with respect to n we deduce the average number of chains n in a micelle

$$n \approx N^{4/5}\sigma^{3/5} \tag{7}$$

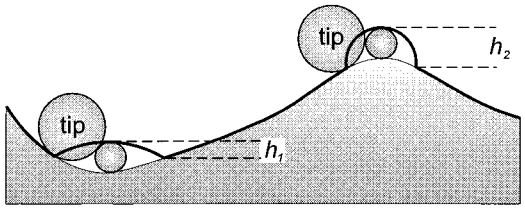

Figure 3. Schematic drawing demonstrating the dependence of the particle shape on the finite tip radius and the local topography of the substrate. The thick line shows the apparent height corrugation. The particle in the valley seems lower and more flattened than the particle on the peak ($h_1 < h_2$).

From eqs 2 and 3 we infer the radius R of the core and the overall size D of a pinned micelle

$$R \approx N^{3/5}\sigma^{1/5} \tag{8}$$

$$D \approx N^{2/5}\sigma^{-1/5} \tag{9}$$

If there is an attractive polymer−surface interaction, the core partially wets the surface. Its shape can be approximated by a spherical cap with a contact angle θ.[27] This angle is a measure of the polymer adsorption onto the substrate. Singh et al.[28] introduced a term which depends on the adsorption energy and on the solvent quality to account for the deformation of the core. This deformation (spreading) does not influence the characteristic exponents of the equations above.

4. Results and Discussion

We have organized this section into two parts: in the first part we present evidence for the transition from single grafted chains to pinned micelles using short and long adsorption times, which result in low and high surface coverages, respectively. In the second part, we investigate the scaling laws that describe the characteristic sizes of the pinned micelles and their cores using PS-SH molecules with different molecular weights.

4.1. Single Chains−Pinned Micelle Transition. In parts a−c of Figure 2 we show a 3D graph, a gray-scale plot, and a line scan, respectively, of a gold substrate that was immersed in a toluene solution of PS_{1400}−SH (0.1 mg/mL) for 45 min. Flat Au terraces separated by valleys and channels can be observed. On these terraces, well-separated collapsed polymer islands can be seen. It appears that these polymer globules are of different sizes. However, our substrate is not completely flat and consequently artifacts are produced: even if two particles are exactly the same, they will be imaged differently if one is on a peak and the other is in a valley, due to convolution of the geometry of the tip and the sample. Figure 3 shows schematically this distortion. Because of this effect, the polymer islands seem to be larger on the peaks and smaller in the valleys. There are a few flat areas, and in these we can see that the islands are similar. We measured the dimensions of the islands and we found an average height and width of 5.5 and 48 nm, respectively. Although the height can be a reliable value, the width due to convolution is overestimated.[29] If we consider that the shape of a polymer island is a spherical cap (the treatment of small globules in terms of macroscopic quantities is justified even for single collapsed polymer coils; for details see ref 27), we can estimate its radius

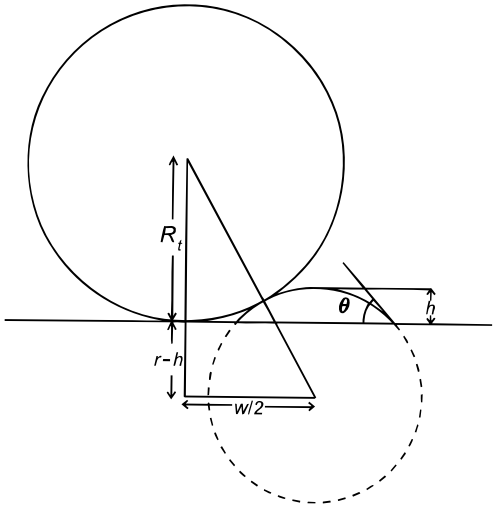

Figure 4. Drawing showing a spherical cap of radius r forming a contact angle θ with the substrate (horizontal line) scanned by a tip of radius R_t. h and w are the measured height and (apparent) width of the spherical cap, respectively. When the substrate is flat, the height is measured correctly but the width is overestimated.

(r) and contact angle (θ) in terms of its apparent width (w), height (h), and tip radius (R_t) (Figure 4):

$$r = \frac{w^2}{8h} + \frac{h}{2} - R_t \tag{10}$$

$$\cos\theta = 1 - \frac{h}{r} \tag{11}$$

We found that the average radius and contact angle are 5.1 nm and 95° ± 15°, respectively. We see that the PS chains are weakly adsorbed on the gold substrate although we would expect otherwise since gold is a high-energy surface. This can be explained by the fact that, during imaging, the whole sample surface is immersed in water, which is a bad solvent for PS and in addition tends to wet clean gold surfaces. From the SFM observations, we estimated the average volume of the globules to be 310 ± 90 nm^3. Theoretically, on the other hand, if one assumes the mass density in a collapsed PS chain to be approximately equal to the usual bulk density for polystyrene (1 g/cm^3), the calculated volume is 239 nm^3, which is close to the volume experimentally found for the globules. Hence, we believe that the globules are isolated single polymer chains chemisorbed and collapsed onto the gold substrate.

Figure 5 shows a gold substrate that has been immersed in the same solution for 24 h. Although the channels that separate the gold islands can still be seen, the flat terraces are covered by a polymer layer. Twenty four hours is adequate time for the adsorption to reach its maximum of about 1 mg/m^2.[19] The corresponding surface density is $\sigma = 0.42 \times 10^{16}\ m^{-2}$. This means that there are about 4×10^3 chains per μm^2. The surprising point is that although the surface coverage has reached its maximum (for this particular concentration), there is a structure of globular objects that are too few in number to be individual chains. We can estimate how close the grafted PS chains are: the surface overlap density σ_{ol} (the surface density where above which the PS buoys will overlap in the adsorbed layer) is $\sigma_{ol} = (\pi R_{PS})^{-2} = 0.16 \times 10^{16}\ m^{-2}$ where $R_{PS} = 0.186 N_{PS}^{0.595} = 14.1$ nm is the radius of gyration of PS in toluene.[30] Since $\sigma > \sigma_{ol}$ the chains overlap with each other. In

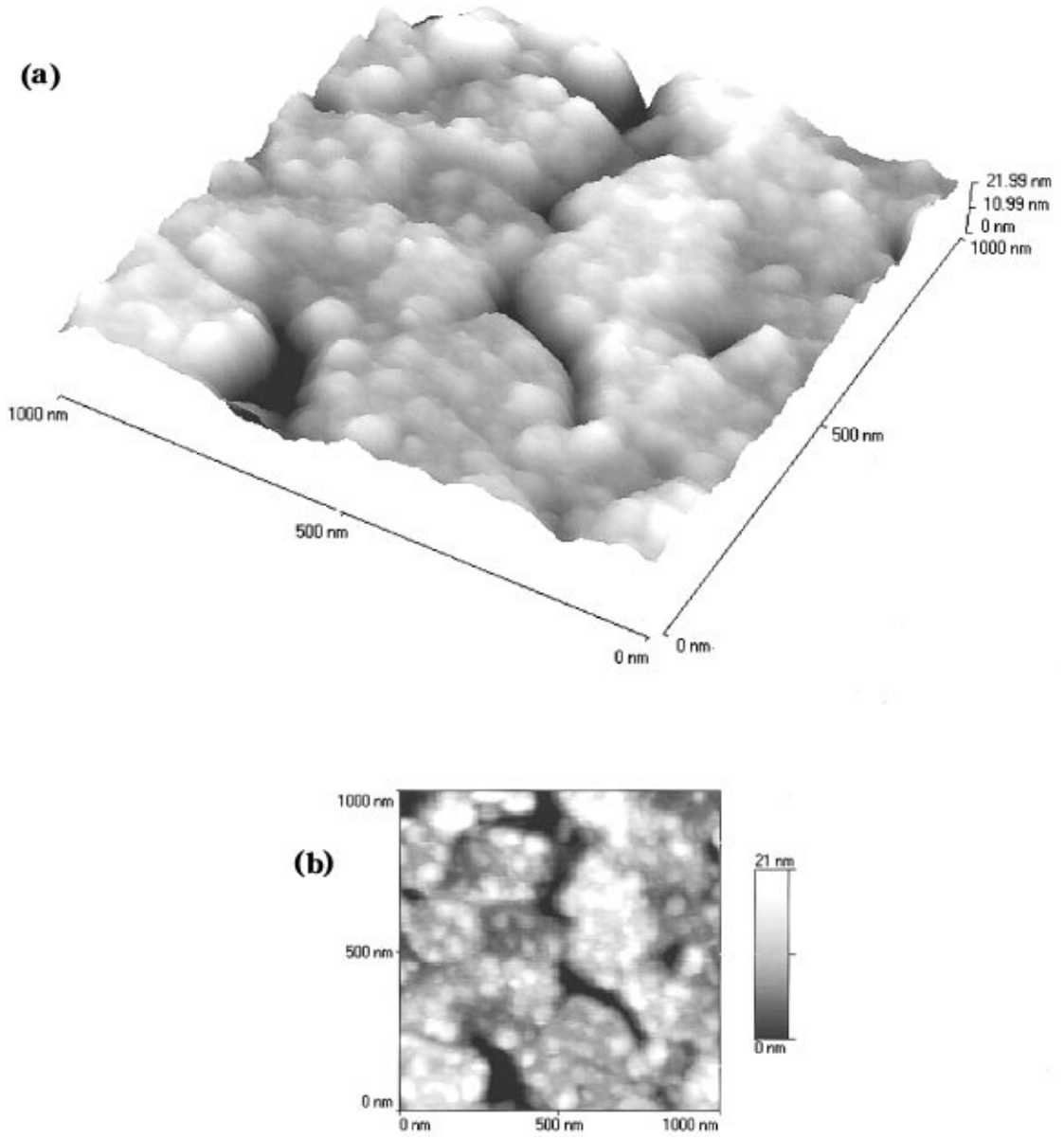

Figure 5. (a) SFM 3D-graph topography image of a gold substrate immersed in a toluene solution of PS_{1400}−SH (concentration, 0.1 mg/mL) for 24 h. Only the top of globules can be seen. (b) Gray scale plot of the same image.

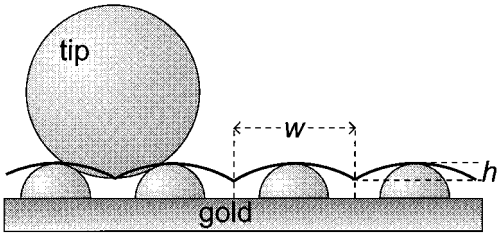

Figure 6. Imaging process of the pinned micelles: only the top of the cores is probed. The width *w* is a measure of the characteristic size of a micelle. The height *h* of the micelles is underestimated.

agreement with the theoretical predictions, the explanation that we propose is that the polymer chains are too close to collapse separately. Instead, they *segregate on a microscale* and form pinned micelles. Since the core of a micelle is a stable, massive structure, it can be probed by the tip of an SFM. In Figure 6 we depict schematically the core of the pinned micelles and the imaging process. In contrast to the previous case of single chains, the pinned micelles are too close for the tip to be able to image the substrate. Deep valleys between the globules are inaccessible and the tip does not probe the gold surface. This produces the smoother corrugation of Figure 5a in comparison with Figure 2a.

4.2. Effect of Molecular Weight on the Size of Micelles. Figure 7 shows samples that have been immersed in solutions that contained PS_x−SH molecules with different molecular weights. In all cases, the gold substrates were kept for 48 h in solutions of 2 mg/mL. It is evident in all images that the polymer layer forms an array of clusters. These clusters are the cores of the pinned micelles that have been formed on the surface. Although there are tip convolution effects, the sizes and distances of the features clearly increase with the molecular weight, in qualitative agreement with eqs 8 and 9.

We concentrate first on the features of Figure 7e: it can be seen from the image and from cross sections (a typical one is the profile (α) in Figure 8) that the polymer globule structure is rather sparse and in most cases the tip scans the gold surface between the micelle cores. We measured the average height, width, and the nearest-neighbor distance of the cores to be 17.6, 96.1, and 109.3 nm, respectively. The nearest neighbor

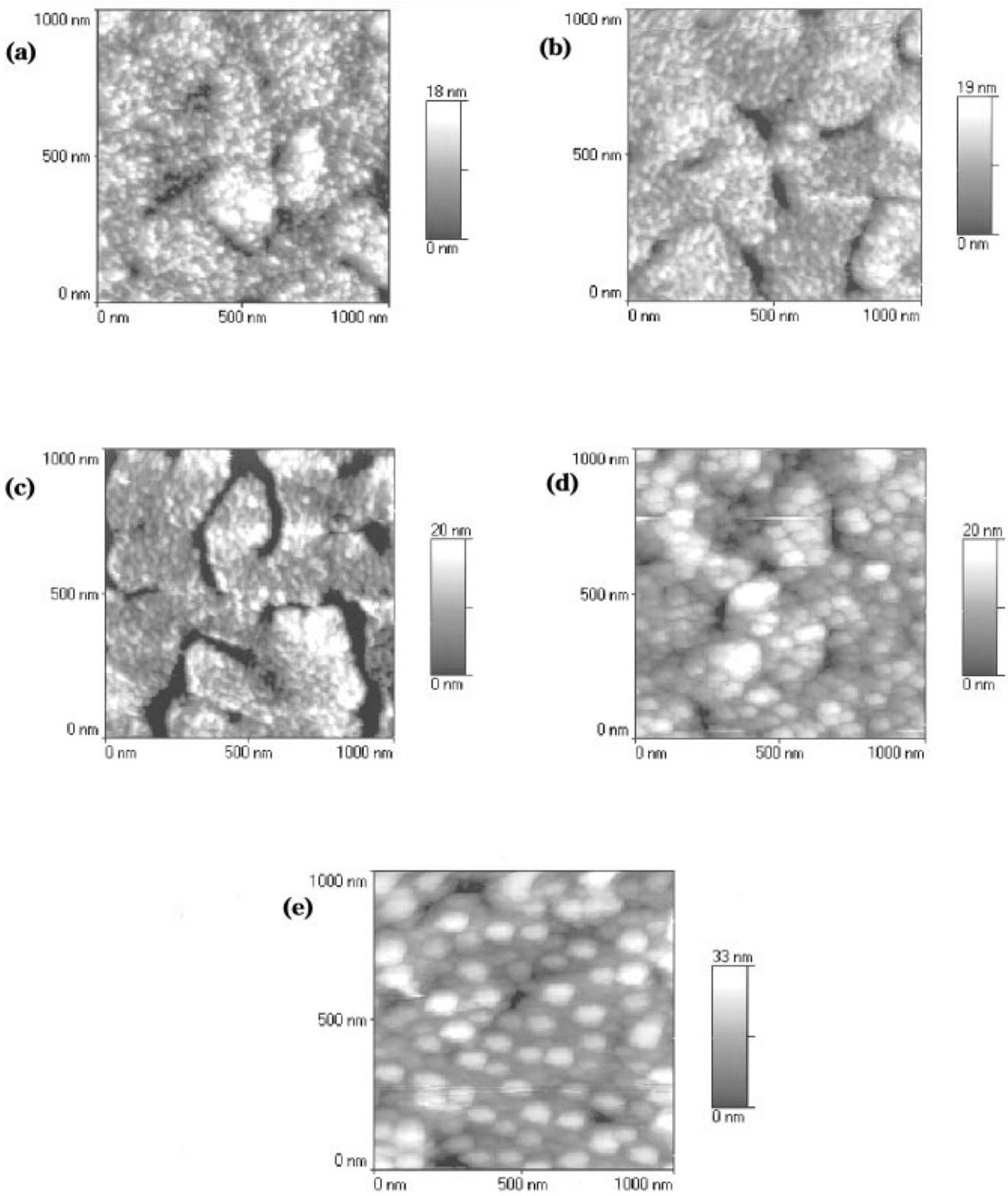

Figure 7. SFM topography images for five different molecular weights: (a) PS_{400}−SH; (b) PS_{500}−SH; (c) PS_{800}−SH; (d) PS_{1400}−SH; (e) PS_{2500}−SH. The sizes of the clusters increase with the molecular weight.

distance is a measure of the characteristic size of a pinned micelle. From eqs 10 and 11 we calculated their average radius and contact angle to be 24.4 nm and 75 ± 10°, respectively. It seems that a relatively big polymer cluster spreads on the surface more than a single polymer globule does. This can be due to the existence of the tethers around the core.

The images a, b, c, and d in Figure 7 are qualitatively similar to the image in Figure 5. The tops of the clusters alone are imaged since the micelle cores are densely distributed. This effect can be clearly seen in cross sections; a typical one is the profile (β) in Figure 8. It looks very similar to the schematic corrugation profile of Figure 6. In this case the average nearest-neighbor distance is approximately equal to the average width of the micelles. We consider the average width as the measure of the characteristic size of a pinned micelle.

We have measured directly from line scans the average width (w), height (h), and the number (N_m) of the pinned micelles (Table 2). We calculated their radii by using eq 10; eq 10 holds for any case in which a

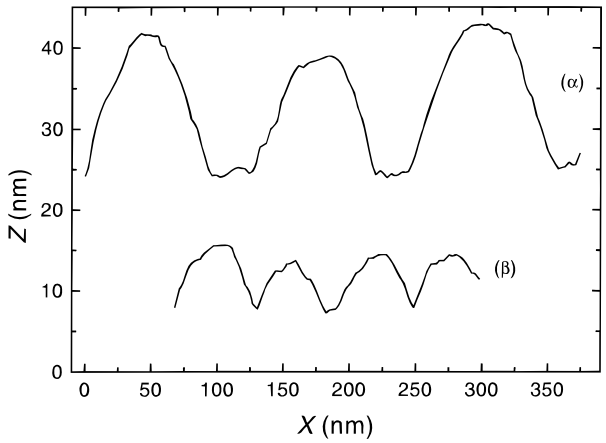

Figure 8. Cross profiles of the cores of pinned micelles. The vertical scaling is different from the horizontal one so the cores appear elongated in the *z* direction. The vertical and horizontal offsets are arbitrary. (α) is from Figure 7e: The cores are sparsely distributed and can be imaged as isolated islands. (*β*) is from Figure 7d: The cores are densely distributed. Due to the finite tip size their top parts alone are probed.

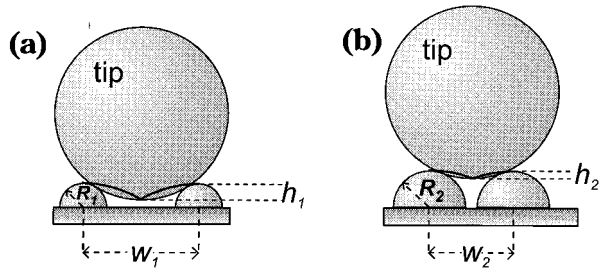

Figure 9. Effect of tip radius and particle surface density on apparent particle size. At relatively small particle separations, particles that are closer look smaller because of the convolution effect: Although the adsorbed globules in (a) are smaller than in (b) ($R_1 < R_2$), the former appear bigger ($w_1 > w_2$) and higher ($h_1 > h_2$).

Table 2. Measured Quantities from SFM Images

M_w	width w (nm)	height h (nm)	no. of micelles on 1 μm^2 N_m
41 500	33.1	2.3	993
51 500	33.9	2.4	949
85 000	43.0	3.7	544
144 000	58.3	6.3	264
258 000	96.1	17.6	97
144 000 (low coverage)	65.8	8.7	152

Table 3. Calculated Quantities for the Pinned Micelles and the Polymer Monolayer

M_w	micelle size D (nm)	core size R (nm)	no. of chains per micelle n	mass coverage Γ (mg/m^2)	$\overline{RD}$ (nm^2)
41 500	33.1	10.7	23	1.57	388.0
51 500	33.9	11.1	21	1.70	373.1
85 000	43.0	14.3	27	2.07	683.0
144 000	58.3	20.6	48	3.03	1274.3
258 000	109.3	24.4	44	1.83	2771.7
144 000 (low coverage)	65.8	16.6	25	0.91	1093.1

spherical top is imaged by a spherical tip. The angles that we calculated from eq 11 for all molecular weights are between 40 and 60°. This can be explained by the above-mentioned fact that the micelle cores are rather close and the tip touches only their upper part, thereby underestimating their height (Figure 6). Consequently, although it was still possible to estimate core radii, we could not measure their contact angles, as we did for the single chains and the large clusters of Figure 7e. However, since the relevant materials are still the same (PS on gold in water), we assumed that the contact angle is 75° for all the molecular weights. We estimated all core volumes, and assuming bulk mass density for the PS globule, we calculated the number of chains (n) that fuse to form one micelle. We also estimated the mass coverage Γ since we know approximately the total number of chains (nN_m) per μm^2. Averages of all calculated values are summarized in Table 3. For Γ we deduced values in the range of 2 mg/m^2, in agreement with published data.[19]

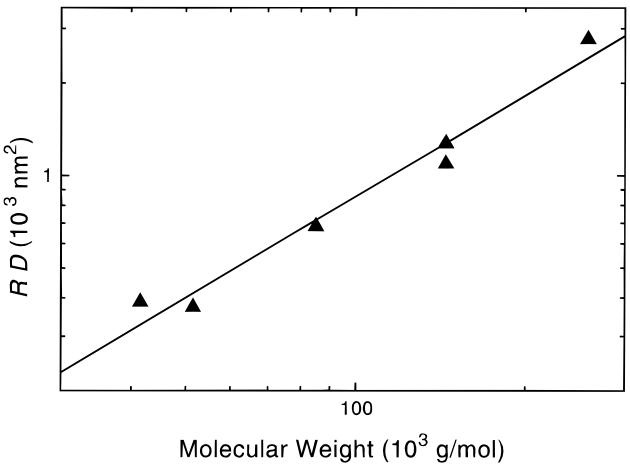

Figure 10. log−log plot of the product RD versus the polymer molecular weight.

For the PS_{1400}−SH polymer we have two images at two different grafting densities (Figure 5a,b, low-density σ_1; Figure 7d, high-density σ_2). We denote the size, core radius, and number of chains of a micelle at low grafting density by D_1, R_1, and n_1, and the corresponding quantities of a micelle in high grafting coverage by D_2, R_2, and n_2, respectively. Since $\sigma_1 < \sigma_2$, we deduce from eqs 8 and 9: $D_1 > D_2$, $R_1 < R_2$. The measured values $D_1 = 65.8$ nm and $D_2 = 58.3$ nm and calculated values $R_1 = 16.6$ nm and $R_2 = 20.6$ nm verify these inequalities. We note also that although the cores of the micelles in Figure 5 look bigger than the ones in Figure 7d, we have deduced the opposite using eq 10. This is due to the fact that the true size of the core depends not only on the apparent width but also on the apparent height which is in the denominator of the first term. Figure 9 illustrates schematically the image formation in both cases.

In the final column of Table 3 we note the average of the product of the core radius with the characteristic size of the pinned micelle $\overline{RD}$ (the product RD was calculated for every particle and these values were averaged). From eqs 8 and 9 we deduce that this product is independent upon the mass coverage and scales as

$$RD \approx N \tag{12}$$

In Table 3 we see that for low- and high-density monolayers of PS_{1400}−SH (Figures 5 and 7d, respectively) the product RD is approximately the same (although their grafting densities are different) as eq 12 predicts. In Figure 10 we present a log−log plot of the product of the core radius with the characteristic size of the pinned micelles versus the molecular weight. We found a slope of 1.09, which is close to the theoretical prediction above (eq 12). The fact that we found a

higher exponent could be due to a higher spreading of the cores with increasing molecular weight. It has to be noted that eq 12, which our results are consistent with, is not an ultimate test of the theory. Equation 12 for *RD* could hold independently of the *exact* functional dependence of separately R and D on N and σ.

5. Conclusions

The spontaneous chemisorption of PS−SH molecules on Au surfaces from a solution in toluene resulted in a monolayer of polymer chains. The monolayers were imaged by SFM in bad-solvent conditions. For very dilute polymer solutions and relatively short incubation times single polymer chains have been identified. The polymer chains were collapsed into globular particles weakly adsorbed on the gold substrate. They were randomly distributed throughout the monolayer and no clustering was observed. When the grafting density was increased by using longer adsorption times, an ordered polymer microstructure was observed. For samples of different molecular weights, arrays of polymer microclusters of different dimensions were observed. We found that the microclusters spread better than the single chain globules and partially wet the gold substrate. We extracted from the SFM images the typical sizes of these microstructures and we found that they are consistent with the scaling laws that were predicted for pinned micelles.

Acknowledgment. We thank Paul van Hutten for the careful reading of this manuscript. This work was supported by the Netherlands Foundation for Fundamental Research on Matter (FOM) and the Netherlands Organization for Scientific Research (NWO).

References and Notes

(1) Napper, D. *Polymeric Stabilization of colloidal Dispersions*; Academic Press: London, 1983.
(2) Gast, A.; Leibler, L. *Macromolecules* **1986**, *19*, 686.
(3) Lee, L. H. *Adhesion and Adsorption of Polymers*; Plenum Press: New York, 1980.
(4) Ruckenstein, E.; Chang, D. B. *J. Colloid Interface Sci.* **1988**, *123*, 170.
(5) Milner, S. T. *Science* **1991**, *251*, 905.
(6) Ross, R. S.; Pincus, P. *Europhys. Lett.* **1992**, *19*, 79.
(7) Yeung, C.; Balazs, A. C.; Jasnow, D. *Macromolecules* **1993**, *26*, 1914.
(8) Tang, H.; Szleifer, I. *Europhys. Lett.* **1994**, *28*, 19.
(9) (a) Lai, P.-Y.; Binder, K. J. *J. Chem. Phys.* **1992**, *97*, 586. (b) Soga, K. G.; Guo, H.; Zuckermann, M. J. *Europhys. Lett.* **1995**, *29*, 531.
(10) Grest, G. S.; Murat, M. *Macromolecules* **1993**, *26*, 3108.
(11) Williams, D. R. M. *J. Phys. II* **1993**, *3*, 1313.
(12) Zhulina, E. B.; Birshtein, T. M.; Priamitsyn, V. A.; Klushin, L. I. *Macromolecules* **1995**, *28*, 8612.
(13) Binnig, G.; Quate, C. F.; Gerber, Ch. *Phys. Rev. Lett.* **1986**, *56*, 930.
(14) O'Shea, S. J.; Welland, M. E.; Rayment, T. *Langmuir* **1993**, *9*, 1826.
(15) Zhao, W.; Krausch, G.; Rafailovich, M. H.; Sokolov, J. *Macromolecules* **1994**, *27*, 2933.
(16) Siqueira, D. F.; Köhler, K.; Stamm, M. *Langmuir* **1995**, *11*, 3092.
(17) Stamouli, A.; Pelletier, E.; Koutsos, V.; van der Vegte, E. W.; Hadziioannou, G. *Langmuir* **1996**, *12*, 3221.
(18) Bain, C. D.; Troughton, E. B.; Tao, Y.-T.; Evall, J.; Whitesides, G. M.; Nuzzo, R. G. *J. Am. Chem. Soc.* **1989**, *111*, 321.
(19) Stouffer, J. M.; McCarthy, T. J. *Macromolecules* **1988**, *21*, 1204.
(20) XPS measurements indicate no adsorption of unmodified polystyrene from a toluene solution onto a gold surface.
(21) Tang, W. T. Study of block copolymer micelles in dilute solution by light scattering and fluorescence spectroscopy. Dissertation, Stanford University, 1987, pp 28−33.
(22) de Gennes, P.-G. *Scaling Concepts in Polymer Physics*; Cornell University Press: Ithaca, NY, 1979.
(23) Koutsos, V.; van der Vegte, E. W.; Pelletier, E.; Hadziioannou, G. To be submitted in *Macromolecules*.
(24) Weisenhorn, A. L.; Hansma, P. K.; Albrecht, T. R.; Quate, C. F. *Appl. Phys. Lett.* **1989**, *54*, 2651.
(25) Burnham, N. A.; Colton, R. J.; Pollok, H. M. *J. Vac. Sci. Technol.* **1991**, *A9*, 2548.
(26) Siedle, P.; Butt, H.-J.; Bamberg, E.; Wang, D. N.; Kühlbrand, W.; Zach, J.; Haider, M. *Inst. Phys. Conf. Ser.* **199***130*, 361.
(27) Johner, A.; Joanny, J. F. *J. Phys. II* **1991**, *1*, 181.
(28) Singh, C.; Zhulina, E. B.; Gersappe, D.; Pickett, G. T.; Balazs, A. C. *Macromolecules*, in press.
(29) Markiewicz, P.; Goh, M. C. *Langmuir* **1994**, *10*, 5.
(30) Higo, Y.; Ueno, N.; Noda, I. *Polym. J.* **1983**, *15*, 367.

MA961625D